DOI: 10.1002/anie.200702505

Lithium Batteries

Nanomaterials for Rechargeable Lithium Batteries**

Peter G. Bruce, Bruno Scrosati, and Jean-Marie Tarascon*

Keywords:
electrochemistry · lithium · nanoelectrodes · nanomaterials · polymers

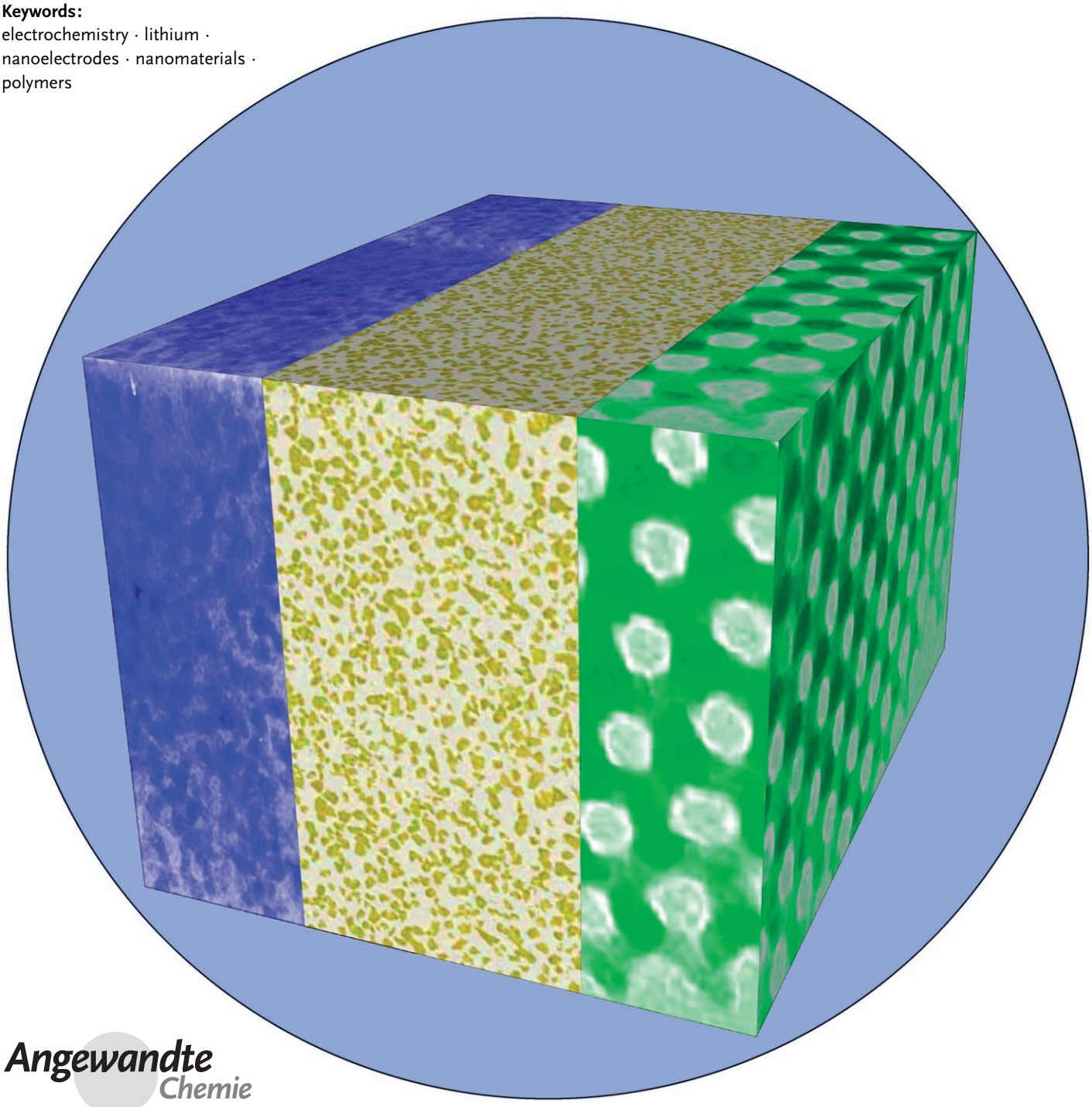

Energy storage is more important today than at any time in human history. Future generations of rechargeable lithium batteries are required to power portable electronic devices (cellphones, laptop computers etc.), store electricity from renewable sources, and as a vital component in new hybrid electric vehicles. To achieve the increase in energy and power density essential to meet the future challenges of energy storage, new materials chemistry, and especially new nanomaterials chemistry, is essential. We must find ways of synthesizing new nanomaterials with new properties or combinations of properties, for use as electrodes and electrolytes in lithium batteries. Herein we review some of the recent scientific advances in nanomaterials, and especially in nanostructured materials, for rechargeable lithium-ion batteries.

From the Contents

1. Introduction

The storage of electrical energy will be far more important in this century than it was in the last. Whether to power the myriad portable consumer electronic devices (cell phones, PDAs, laptops, or for implantable medical applications, such as artificial hearts, or to address global warming (hybrid electric vehicles, storage of wind/solar power), the need for clean and efficient energy storage will be vast. Nanomaterials have a critical role to play in achieving this change in the way we store energy.

Rechargeable lithium batteries have revolutionized portable electronic devices. They have become the dominant power source for cell phones, digital cameras, laptops etc., because of their superior energy density (capability to store 2–3 times the energy per unit weight and volume compared with conventional rechargeable batteries). The worldwide market for rechargeable lithium batteries is now valued at 10 billion dollars per annum and growing. They are the technology of choice for future hybrid electric vehicles, which are central to the reduction of CO_2 emissions arising from transportation.

The rechargeable lithium battery does not contain lithium metal. It is a lithium-ion device, comprising a graphite negative electrode (anode), a non-aqueous liquid electrolyte, and a positive electrode (cathode) formed from layered $LiCoO_2$ (Figure 1). On charging, lithium ions are deintercalated from the layered $LiCoO_2$ intercalation host, pass across the electrolyte, and are intercalated between the graphite layers in the anode. Discharge reverses this process. The electrons, of course, pass around the external circuit. The rechargeable lithium battery is a supreme representation of solid-state chemistry in action. A more detailed account of lithium-ion batteries than is appropriate here may be obtained from the literature.[1–3]

The first-generation lithium-ion battery has electrodes that are composed of powders containing millimeter-sized particles, and the electrolyte is trapped within the millimeter-sized pores of a polypropylene separator. Although the battery has a high energy density, it is a low-power device (slow charge/discharge). No matter how creative we are in designing new lithium intercalation hosts with higher rates, limits exist because of the intrinsic diffusivity of the lithium ion in the solid state (ca. 10^{-8} $cm^2 s^{-1}$), which inevitably limits the rate of intercalation/deintercalation, and hence charge/discharge. However, an increase in the charge/discharge rate of lithium-ion batteries of more than one order of magnitude is required to meet the future demands of hybrid electric vehicles and clean energy storage. Nanomaterials, so often

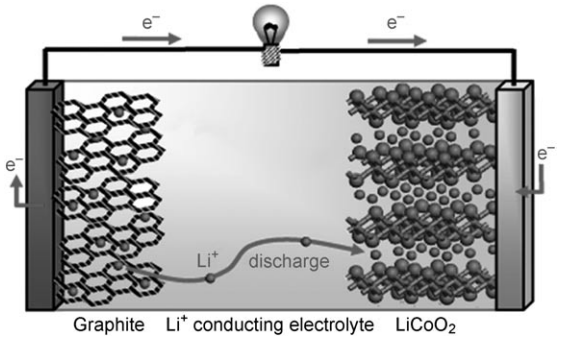

Figure 1. Schematic representation of a lithium-ion battery. Negative electrode (graphite), positive electrode ($LiCoO_2$), separated by a non-aqueous liquid electrolyte.

[*] Prof. P. G. Bruce
School of Chemistry
University of St. Andrews
St. Andrews, Fife, KY16 9ST (UK)
Fax: (+44) 1334-463808
E-mail: p.g.bruce@st-andrews.ac.uk
Prof. B. Scrosati
Dipartimento di Chimica
Università di Roma
Rome (Italy)
Prof. J.-M. Tarascon
Laboratoire de Reactivite et de Chimie des Solides
Universite de Picardie
Amiens (France)

[**] Thanks to Dr. Aurelie Debart for preparation of the frontispiece.

hyped or misrepresented by claims of delivering new properties, have the genuine potential to make a significant impact on the performance of lithium-ion batteries, as their reduced dimensions enable far higher intercalation/deintercalation rates and hence high power. This is just one property that may be enhanced by the use of nanomaterials. However, nanomaterials are certainly not a panacea. The advantages and disadvantages of lithium-ion battery materials are summarized in Section 2, and thereafter advances in the use of nanomaterials, emphasizing in particular nanostructured materials, as negative electrodes, electrolytes, and positive electrodes for rechargeable lithium batteries are described.[4] The illustrative examples that are presented are mainly from the work of the authors.

2. Advantages and Disadvantages of Nanomaterials for Lithium Batteries

Advantages

1. They enable electrode reactions to occur that cannot take place for materials composed of micrometer-sized particles; for example, reversible lithium intercalation into mesoporous β-MnO_2 without destruction of the rutile structure.[5]
2. The reduced dimensions increases significantly the rate of lithium insertion/removal, because of the short distances for lithium-ion transport within the particles. The characteristic time constant for diffusion is given by $t = L^2/D$, where L is the diffusion length and D the diffusion constant. The time t for intercalation decreases with the square of the particle size on replacing micrometer with nanometer particles.[4]
3. Electron transport within the particles is also enhanced by nanometer-sized particles, as described for lithium ions.[4]
4. A high surface area permits a high contact area with the electrolyte and hence a high lithium-ion flux across the interface.
5. For very small particles, the chemical potentials for lithium ions and electrons may be modified, resulting in a change of electrode potential (thermodynamics of the reaction).[6]
6. The range of composition over which solid solutions exist is often more extensive for nanoparticles,[7] and the strain associated with intercalation is often better accommodated.

Disadvantages

1. Nanoparticles may be more difficult to synthesize and their dimensions may be difficult to control.
2. High electrolyte/electrode surface area may lead to more significant side reactions with the electrolyte, and more difficulty maintaining interparticle contact.
3. The density of a nanopowder is generally less than the same material formed from micrometer-sized particles. The volume of the electrode increases for the same mass of material thus reducing the volumetric energy density.

Peter Bruce is Professor of Chemistry at the University of St Andrews, Scotland. His research interests embrace the synthesis and characterization of materials (extended arrays and polymers) with new properties or combinations of properties, and in particular materials for new generations of energy conversion and storage devices. He has received a number of awards and fellowships, and is a fellow of the Royal Society.

Bruno Scrosati is Professor of Electrochemistry at the University of Rome. He has been president of the International Society of Solid State Ionics, the Italian Chemical Society, and the Electrochemical Society, and is fellow of the Electrochemical Society (ECS) and of the International Society of Electrochemistry (ISE). He has a "honoris causa" (honorary DSc) from the University of St. Andrews in Scotland. He won the XVI Edition of the Italgas Prize, Science and Environment. He is European editor of the Journal of Power Sources and member of the editorial boards of various international journals.

Jean-Marie Tarascon is Professor at the University of Picardie (Amiens). He develops techniques for the synthesis of electronic materials (superconductors, ferroelectrics, fluoride glasses, and rechargeable batteries) for new solid-state electronic devices. He played a pivotal role in the development of a thin and flexile plastic lithium-ion battery that is presently being commercially developed. He is investigating new lithium reactivity concepts, and electrodes for the next generation of lithium-ion batteries. He is the founder of ALISTORE.

3. Negative Electrodes

3.1. Nanoparticles

Graphite powder, composed of micrometer-sized particles, has been the stalwart of negative electrodes for rechargeable lithium batteries for many years.[1,2] Replacement by nanoparticulate graphite would increase the rate of lithium insertion/removal and thus the rate (power) of the battery. Lithium is inserted into graphite at a potential of less than 1 V versus Li^+/Li. At such low potentials, reduction of the electrolyte occurs, accompanied by the formation of a passivating (solid electrolyte interface) layer on the graphite surface.[8–10] The formation of such a layer is essential for the operation of graphite electrodes, as it inhibits exfoliation. The severity of layer formation would, in the case of high-surface-area nanoparticulate graphite, result in the consumption of excessive charge, which would then be lost to the cell. Of even greater importance is the fact that most of the lithium is intercalated into graphite at potentials of less than 100 mV versus Li^+/Li; were it not for careful electronic control of charging, lithium could deposit on the graphite surface. The deposition of highly reactive lithium would be serious for

micrometer-sized particles, but could be catastrophic for nanosized particles, leading to major safety concerns. In short, increasing the rate capability of lithium batteries by using nanoparticulate graphite presents formidable problems.

3.2. Nanotubes/wires

Given the significance of C_{60} and carbon nanotubes, it is apposite to start with a comment on their potential use as negative electrodes in lithium batteries. Several investigations have been carried out on these materials as electrodes.[11,12] Although lithium intercalation is possible, and carbon nanotubes exhibit twice the lithium storage compared with graphite, similar problems of surface-layer formation and safety are present. Carbon nanotubes do not seem to offer a major route to improved electrodes. In the search for alternatives to graphite that combine inherent protection against lithium deposition, with low cost, low toxicity, and the ability to be fabricated as a nanomaterial delivering fast lithium insertion/removal, attention has focused recently on titanium oxides. The defect spinel $Li_4Ti_5O_{12}$ ($Li[Li_{1/3}Ti_{5/3}]O_4$) is an intercalation host for lithium that may be cycled over the composition range $Li_{4+x}Ti_5O_{12}$, $0 < x < 3$ (Figure 2).[13,14] Intercalation

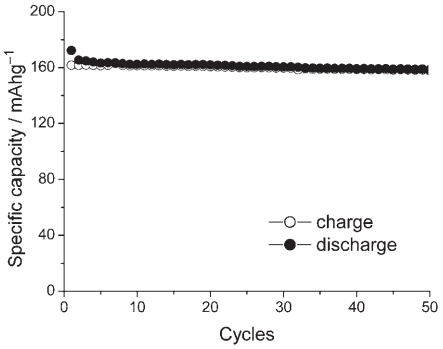

Figure 2. Variation of charge (lithium) stored in a $Li_4Ti_5O_{12}$ intercalation electrode on cycling (intercalation/deintercalation) at a rate of $C/5$ (charge/discharge of cell capacity C in 5 h).

occurs at a potential of about 1.5 V versus Li^+/Li, thus the potential problem of lithium deposition is alleviated, rendering the material significantly safer than graphite. $Li_4Ti_5O_{12}$ is non-toxic and when fabricated as nanoparticles gives high rates of lithium insertion/removal owing to the short diffusion distances in the nanoparticles.[13,14] Based on these advantages, prototype lithium batteries have been constructed using nanoparticulate $Li_4Ti_5O_{12}$ in place of graphite (Figure 3).[15] However, the capacity to store lithium is only half that of graphite, 150 mA h g^{-1} compared with 300 mA h g^{-1}. This fact, combined with the reduced cell voltage because of the increased potential of the negative electrode, namely 0 to 1.5 V, leads to a reduced energy density.

Nanotubes/nanowires composed of TiO_2-(B), the fifth polymorph of titanium dioxide, retain the advantages of $Li_4Ti_5O_{12}$: low cost, low toxicity, high safety, and an electrode potential that eliminates lithium plating. Furthermore, the

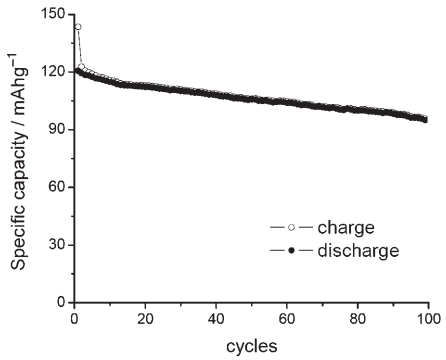

Figure 3. Cycling of a $Li_4Ti_5O_{12}$/GPE/$LiMn_2O_4$ lithium-ion polymer battery. GPE: $LiPF_6$-PC-EC-PVdF gel electrolyte; PC = propylene carbonate, EC = ethylene carbonate, PVdF = poly(vinylidene fluoride). Charge-discharge rate: $C/5$.

amount of lithium that may be stored increases from 150 mA h g^{-1} to 300 mA h g^{-1}, and this increased storage can be delivered at similar high rates to $Li_4Ti_5O_{12}$.[16–18]

The crystal structure of TiO_2-(B) (space group $C2/m$) is composed of edge- and corner-sharing TiO_6 octahedra that form Perovskite-like windows between sites, which leads to facile lithium-ion intercalation. The crystal structure and transmission electron spectroscopy (TEM) images of TiO_2-(B) wires and tubes are shown in Figure 4. Lithium-ion diffusion is primarily in two dimensions, with the planes being orientated at right angles to the axis of the wires, ensuring fast lithium-ion insertion/removal owing to the small 20–40-nm diameter of the wires. The TiO_2-(B) nanowires exhibit higher reversibility of intercalation (> 99.9 % per cycle, after the first cycle) than nanoparticles of TiO_2-(B), even when the size of the particles is the same as the diameter of the wires (Figure 5). The wires, typically 0.1–1 mm long, need only

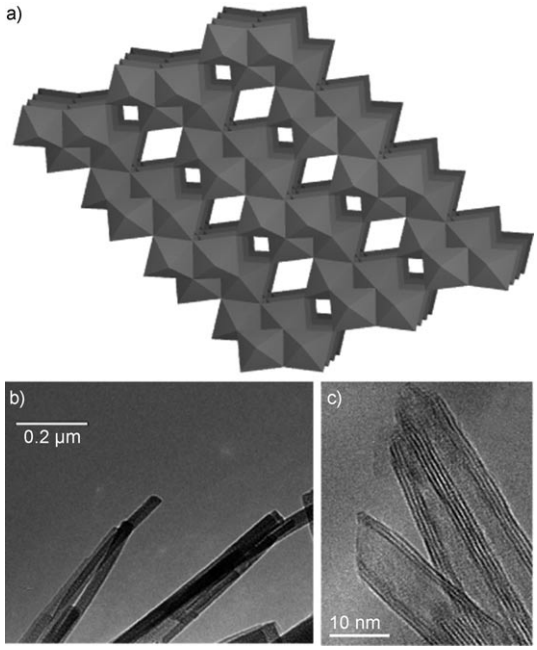

Figure 4. a) Crystal structure of TiO_2-B, TEM images of TiO_2-B b) nanowires and c) nanotubes.

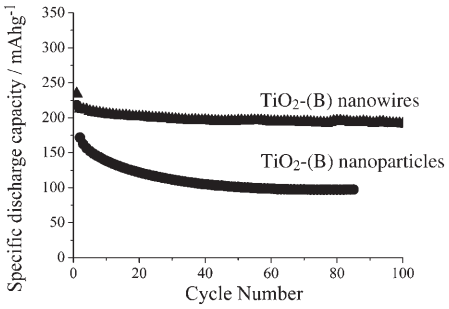

Figure 5. Charge (lithium) stored in the intercalation hosts, TiO_2-B nanowires and nanoparticles, on cycling (intercalation/deintercalation) at a rate of 50 mAg^{-1} (ca. *C*/4). The size of the nanoparticles is the same as the diameter of the nanowires.

make a few points of contact to ensure electron transport, whereas nanoparticles may easily become disconnected as the particles expand and contract on charge/discharge. This result serves to illustrate the importance of controlling the dimensions of nanostructured materials to optimize performance: one long (millimeter) dimension ensures good electron transport between the wires, and two short (nanometer) dimensions ensure fast lithium-ion insertion/removal. The potential at which insertion/removal takes place is the same for bulk, nanoparticulate, and nanowire TiO_2-(B), suggesting that 20 nm is not sufficiently small to influence the energetics of lithium intercalation. However, TiO_2-(B) tubes in which intercalation occurs within a wall thickness of 25–30 Å, exhibit small 5—20-mV deviations from the potential observed for the wires. When incorporated into lithium-ion cells, the TiO_2-(B) nanowires exhibit excellent performance (Figure 6).[19] TiO_2-(B) is not the only nanowire electrode of interest; other examples, including Sn, Co, and V oxides, have been reported.[20–22]

3.3. Nanoalloys

Owing to their ability to store large amounts of lithium, lithium metal alloys, Li_xM_y, are of great interest as high capacity anode materials in lithium-ion cells. Such alloys have specific capacities which exceed that of the conventional graphite anode; for example, $Li_{4.4}Sn$ (993 mA h g^{-1} and 1000 mA h cc^{-1} versus 372 mA h g^{-1} and 855 mA h cm^{-3} for graphite), and $Li_{4.4}Si$ (4200 mA h g^{-1} and 1750 mA h cm^{-3}). Unfortunately, the consequence of accommodating such a large amount of lithium is large volume expansion–contraction that accompanies their electrochemical alloy formation. These changes lead rapidly to deterioration of the electrode (cracks, and eventually, pulverization), thus limiting its lifetime to only a few charge–discharge cycles. Significant research effort has been devoted to overcome this problem. One of the earliest approaches involved replacing bulk material with nanostructured alloys.[23,24] Reducing the metal particles to nanodimensions does not of course reduce the extent of volume change but does render the phase transitions that accompany alloy formation more facile, and reduces cracking within the electrode.[4]

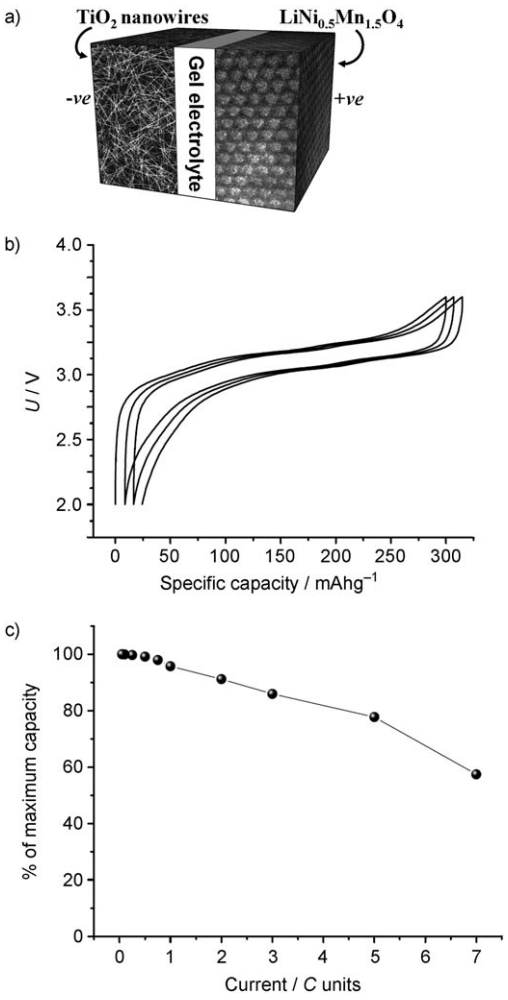

Figure 6. a) Schematic representation of a lithium-ion battery with TiO_2-B nanowires as the negative electrode and $LiNi_{1/2}Mn_{3/2}O_4$ spinel as the positive electrode. b) Variation of voltage on charge-discharge of the cell shown in (a) at a rate of *C*/5. c) Variation of charge stored (lithium) as a function of charge/discharge (intercalation/deintercalation) rate, expressed in terms of percentage of the maximum capacity obtained at low rate for the cell shown in (a).

Different synthetic routes have been used to fabricate nanostructured metals that can alloy with lithium, including sol–gel, ball-milling, and electrodeposition.[25–27] Of these routes, electrodeposition is the most versatile, as it permits easy control of the electrode morphology by varying the synthesis conditions, such as current density and deposition time.

Figure 7 shows tin electrodeposited on a copper foil substrate under different conditions.[28] Their electrochemical behavior in lithium cells is shown in Figure 8.[28] Thus, by selecting a suitable morphology, the performance of the metal alloy electrodes may be enhanced in comparison with that offered by conventional, bulk materials. For instance, good cycle life (>300 cycles) has been demonstrated for a metal electrode based on silicon nanoparticles by Sanyo. Although nanoalloys can cycle lithium better then the equivalent bulk materials, they are unable to sustain the hundreds of cycles necessary for application in a rechargeable battery. The

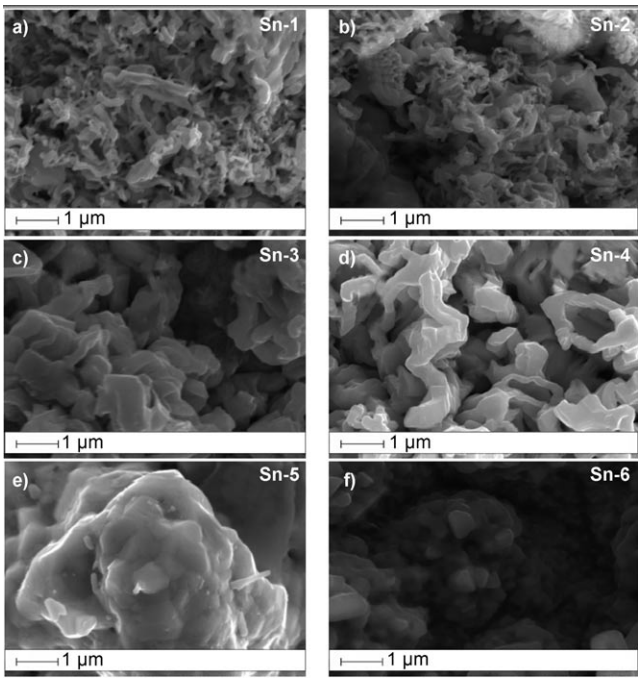

Figure 7. Scanning electron microscopy (SEM) images of various tin samples prepared under different electrodeposition conditions a) 0.5 $mA\,cm^{-2}$; 60 min; b) 1.0 $mA\,cm^{-2}$; 30 min; c) 2.0 $mA\,cm^{-2}$; 15 min; d) 3.0 $mA\,cm^{-2}$; 10 min ; e) 6.0 $mA\,cm^{-2}$; 5 min; f) 15 $mA\,cm^{-2}$; 2 min.

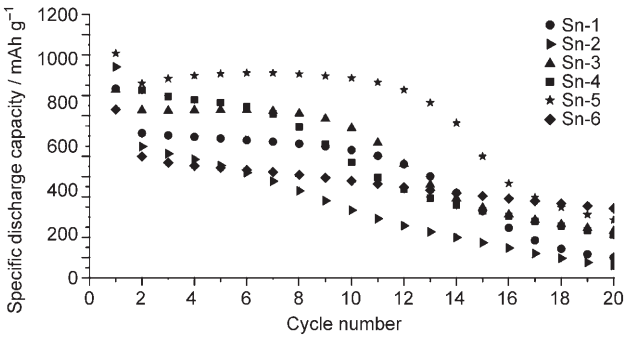

Figure 8. Specific discharge capacity versus cycle number for lithium cells using samples Sn-1, Sn-2, Sn-3, Sn-4, Sn-5, and Sn-6 (see Figure 7.), respectively, in EC:DMC 1:1 $LiPF_6$ electrolyte. Charge–discharge current density: 1 $A\,cm^{-2}\,g^{-1}$, rate: ca. 0.8 *C*. For the identification of the samples, see Figure 7.

volume changes exceed 200–300 %, and reduction of the particle size alone is insufficient. Thus, further optimization is needed to make these materials of practical use.

One approach is to increase the free space which may accommodate the volume variations. This approach has been investigated by designing revolutionary nanoarchitectured electrodes. An early example is a silicon electrode prepared in the form of nanopillars by etching bulk substrates.[29] The nanopillars are sufficiently separated to offer free space to accommodate their expansion during lithium uptake. An alternative approach involves replacing the single metal alloy with an AB intermetallic phase, for which the electrochemical process in a lithium cell involves the displacement of one metal, e.g., B, to form the desired lithium alloy, Li_xB, while the other metal, A, acts as an electrochemically inactive matrix to buffer the volume variations during the alloying process. For instance, the electrochemical reaction for the intermetallic Ni_3Sn_4 is expected to involve a initial activation step [Equation (1)] followed by the main, reversible, electrochemical process [Equations (2) and (3)].

$$Ni_3Sn_4 + 17.6\,Li^+ + 17.6\,e^- \rightarrow 4\,Li_{4.4}Sn + 3\,Ni \quad (1)$$

$$Li_{4.4}Sn \rightarrow Sn + 4.4\,Li^+ + 4.4\,e^- \ (\text{charge}) \quad (2)$$

$$Sn + 4.4\,Li^+ + 4.4\,e^- \rightarrow Li_{4.4}Sn \ (\text{discharge}) \quad (3)$$

Whereas the first step is irreversible, the subsequent steps are reversible and represent the steady-state electrochemical operation of the electrode, with a theoretical capacity of 993 $mA\,h\,g^{-1}$, calculated on the basis of the reversible electrochemical process alone.

By fabricating intermetallic electrodes as nanoparticles, promising results have been obtained.[30] However, even better rate and reversibility has been achieved by using a nanoarchitectured configuration, such as that obtained by a template synthesis.[31] Basically, this procedure involves the use of a nanoarchitectured copper current collector, prepared by growing an array of copper nanorods of about 200 nm in diameter onto a copper foil by electrodeposition through a porous alumina membrane, which is subsequently dissolved. The synthesis is then completed by coating the copper nanorod array with the intermetallic Ni_3Sn_4 particles.[32a]

Figure 9 clearly shows that the Ni_3Sn_4 nanoparticles (of the order of 50 nm) are uniformly deposited on the surface of the copper nanorods, without any coalescence between them. Figure 10 shows the cycling response of this electrode in a lithium cell: the capacity to store lithium is maintained at high values for hundreds of cycles, with no sign of any significant decay. Examination of the electrode cycling showed no evidence of an appreciable change in the morphology (Figure 11). The volume variations upon cycling are effectively buffered by the large free volume between the pillars, thus giving rise to the excellent capacity retention.

Others have emphasized the advantage of using amorphous nanostructured alloys because of their isotropic

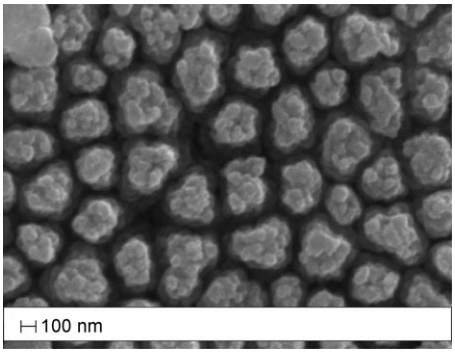

Figure 9. SEM image showing a top view of Ni_3Sn_4 electrodeposited on a copper–nanorod current collector.

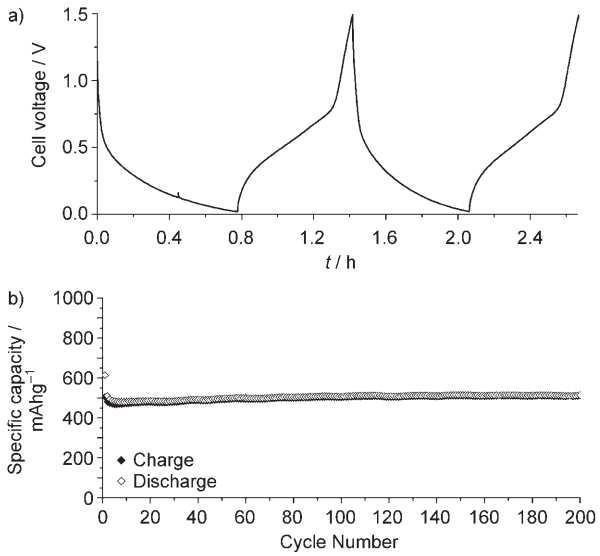

Figure 10. a) Voltage profiles of the first two cycles and b) capacity delivered upon cycling of nanostructured Ni_3Sn_4 used as the electrode in a lithium cell.

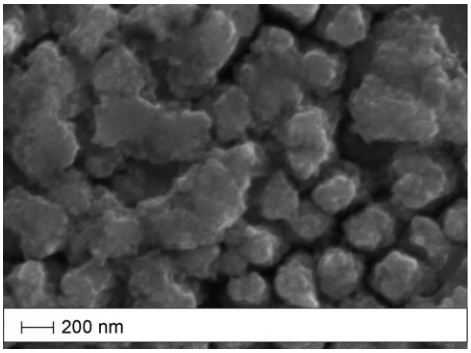

Figure 11. SEM image of the top view of the nanostructured Ni_3Sn_4 electrode after cycling as shown in Figure 10. No evidence of any appreciable change in the morphology is apparent (compare Figure 9). From reference [26].

expansion/contraction and the important role of the binder in the composite electrode in immobilizing the particles and maintaining the integrity of the electrode. The work of Dahn et al. must be mentioned in this context.[32b]

Sony recently introduced a new lithium-ion battery, tradenamed Nexelion, in which for the first time in a commercial cell, the graphite electrode is replaced with an alloy. It operates with a stable capacity for hundreds of cycles.[33,34] Although the information on the composition of the alloy is still scarce, it appears to be based on tin, cobalt, and carbon, with small amounts of titanium proving to play an important role. This development will doubtless open a new chapter on alloy and nanoalloy electrodes in lithium batteries.

3.4. Displacement Reactions

In Section 3.3, the concept of displacing one metal A from a binary intermetallic AB by lithium reduction, with the end result being the formation of a composite containing the displaced metal A together with the alloy Li_xB was described. Instead, intermetallics may be formed, in which one metal is displaced when lithium is inserted into the other.[35] This approach depends on selecting intermetallic alloys such as Cu_6Sn_5, InSb, and Cu_2Sb that show a strong structural relationship with their lithiated products; for example Li_2CuSn and Li_3Sb have structures that are related to Cu_6Sn_5 and InSb, respectively.[36] In the case of InSb and Cu_2Sb for example, as lithium is inserted, copper or indium are extruded as nanoparticles from an invariant face-centred-cubic antimony subarray Figure 12.[37] The stable antimony

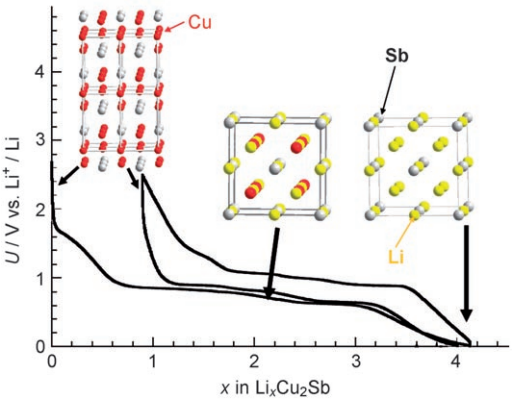

Figure 12. The voltage composition curve for Li/Cu_2Sb, with the structural evolution upon cycling so as to emphasize both the copper extrusion/reinjection upon cycling together with the maintenance of the antimony array.

array provides a host framework for the incoming and extruded metal atoms, thereby limiting the volume expansion. For instance, in the ternary $Li_xIn_{1-y}Sb$ system ($0 < x < 3$, $0 < y < 1$), the antimony array expands and contracts isotropically by only 4%, whereas the overall expansion of the electrode is 46% if the extruded indium is taken into account. For comparison, it should be recalled that 200–300% volume expansion occurs on fully lithiating tin ($Li_{4.4}Sn$) or silicon ($Li_{4.4}Si$). However this elegant new concept still suffered from poor cyclability, although recently, by forming nanoparticles coated with a conductive carbon film,[38] Cu_2Sb electrodes, capable of sustaining capacities as high as 300 $mA\,h\,g^{-1}$ for more than 300 cycles have been demonstrated.

Although not a negative electrode, it has recently been reported that $Cu_{7/3}V_4O_{11}$ reacts electrochemically with lithium through a reversible copper displacement–insertion reaction, leading upon discharge to the extrusion of nanometric or micrometric metallic copper, depending on the discharge rate.[39] With a reacting voltage of 2.7 V, this material is a positive electrode. Through a survey of numerous copper-based materials it was concluded that Cu^+ mobility together with a band structure that locates the $Cu^{1+/0}$ redox couple close to that of the host is essential in designing materials that undergo such displacement reactions.

3.5. Conversion Reactions

Processes based on intercalation/deintercalation are inevitably limited in capacity to one or at most two lithium atoms per host, hence the interest in alloy negative electrodes described in Section 3.3. Seeking other examples of lithium in the solid state that are not constrained by the requirements of intercalation, it has been shown that lithium can react with a range of transition-metal oxides by a process termed conversion.

For example, the simple binary transition metal oxides with the rock salt structure (CoO, CuO, NiO, FeO) having no free voids to host lithium and metallic elements (Co, Cu, Ni, or Fe) do not form alloys with lithium; however they can react reversibly with lithium according to the general reaction $MO + 2\,Li^+ + 2\,e^- \rightleftharpoons Li_2O + M^0$.[40] Their full reduction leads to composite materials consisting of nanometric metallic particles (2–8 nm) dispersed in an amorphous Li_2O matrix (Figure 13). Owing to the nanometric nature of this composite, such reactions were shown to be highly reversible, providing outstanding capacities to store lithium (four times those of commonly used graphite materials) and these capacities can be maintained for hundreds of cycles (Figure 14).

The conversion reaction turns out to be widespread; since the original discovery, many other examples of conversion reactions including sulfides, nitrides, fluorides, and phosphides have been reported.[41–47] They have been shown to involve, depending on the oxidation state of the 3d metal, one (Cu_2O), two (CoO), three (Fe_2O_3), or four (RuO_2) electrons per 3d metal, thus offering the possibility of achieving negative electrodes with high capacity improvements over the existing ones, while using low-cost elements, such as manganese or iron. Another advantage of such conversion reactions lies in the internally nanostructured character of the electrode that is created during the first electrochemical reduction. Because of the internal nanostructure rather than individual nanoparticles, low-packing densities associated with the latter do not exist. Furthermore, the chemical

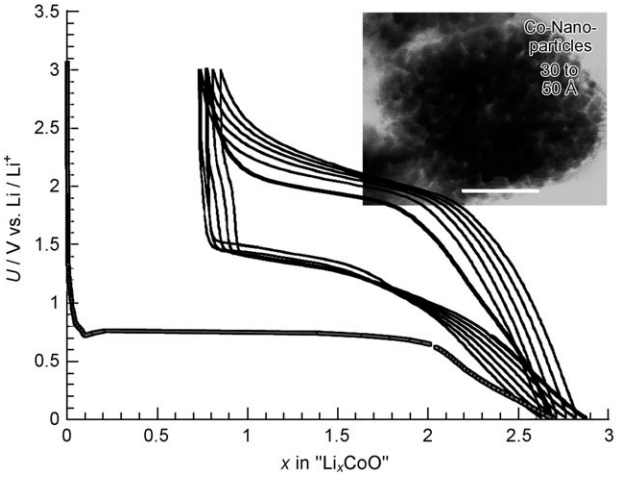

Figure 13. Voltage composition profile for a CoO/Li cell with a TEM image of a CoO electrode recovered from a CoO/Li cell that was fully discharged.

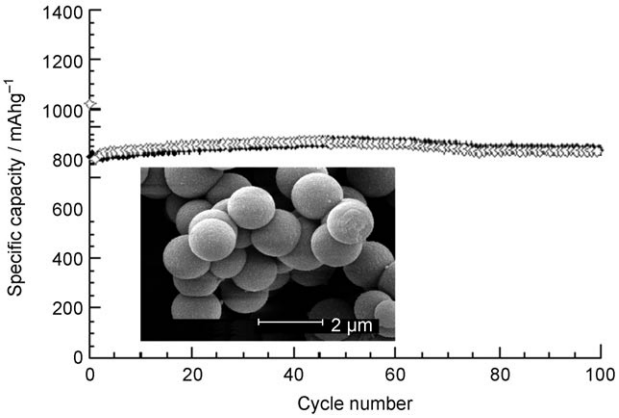

Figure 14. Capacity retention of a Co_3O_4/Li cell together with a SEM image (inset) showing the spherical precursor particles.

versatility of such conversion reactions provides a unique opportunity to control the redox potential by tuning the electronegativity of the anion. Thus the feasibility of using conversion reactions to design either negative (phosphides, nitrides, or oxides) or positive (fluoride) electrodes arises. Fluoride-type compounds were illustrated by G. Amatucci's recent work on compounds such as FeF_3[44] or BiF_3.[45] They have shown that these fluorides are reversible, reacting with three equivalents of lithium at 2.5 V, leading to energy densities as high as 800 mW h g^{-1} of material.[44,45] Unfortunately, such fluoride phases are lithium-free and therefore not suitable for today's lithium-ion cells, for which the only source of lithium is in the as-prepared positive electrode material. However, mixtures of LiF and iron have been prepared and demonstrated in lithium-ion cells.

A major drawback of conversion reactions is their poor kinetics (that is, the rate at which lithium ions and electrons can reach the interfacial regions within the nanoparticle and react with the active domains). This drawback manifests itself as a large separation of the voltage on charge and discharge (large ΔE), implying poor energy efficiency of the electrodes.[48,49] This polarization may be associated with the energy barrier to trigger the breaking of the M–X bonds and was shown to be sensitive to the nature of the anion, decreasing from $\Delta E \cong 0.9$ V to $\cong 0.4$ V on moving from an oxide to a phosphide (Figure 15).[50] The low polarization and low voltage of the phosphides has made compounds such as FeP_2 and NiP_2 attractive as negative electrodes, and especially NiP_2, which can reversibly react with six electrons per nickel atom. If the problem of stability in contact with the electrolyte could be solved then this material would be a great alternative to graphite.

Recognizing that the transport of lithium ions and/or electrons limits the kinetics of conversion reactions, a nanostructured approach has been taken to reduce the diffusion distances. Self-supported nanoarchitectured electrodes, such as Cr_2O_3 layers on stainless-steel substrates by a specific thermal treatment, NiP_2 layers by vapor-phase transport on a commercial nickel foam commonly used in nickel-based alkaline batteries (Figure 16), and electrochemically plated Fe_3O_4 on a copper–nanorod alloy, have all been prepared to

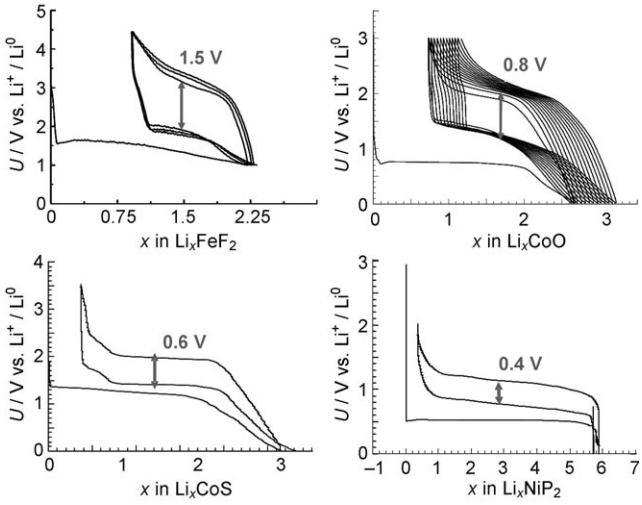

Figure 15. Voltage composition traces for various binary phases belonging respectively to the fluoride, oxide, sulfide, and phosphide families.

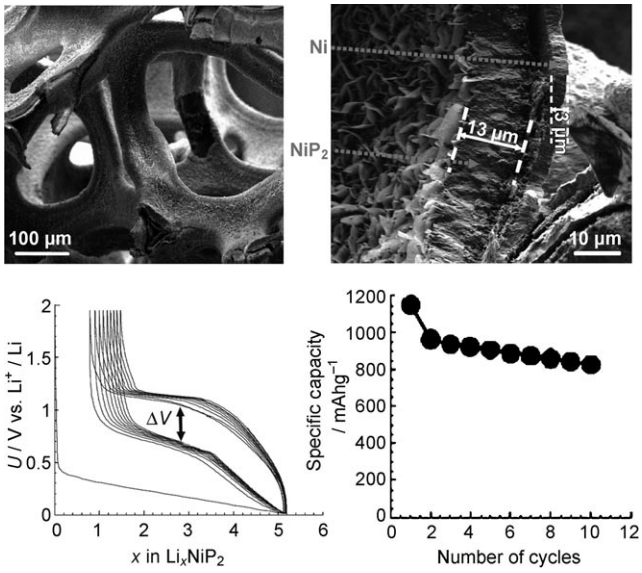

Figure 16. Above: SEM view of a commercial nickel foam prior to (left) and after (right) reaction with phosphorus. Below: the voltage profile (left) and capacity retention (right) of the self-supported NiP_2 electrode.

address the problem of kinetics.[49,51,52] Overall, whatever the electrode design, outstanding rate capability can be achieved despite the separation of charge and discharge potential remaining high. Thus, conversion electrodes can simultaneously show large polarization and fast kinetics. This effect is quite unusual and distinct from intercalation electrodes.

4. Electrolytes

4.1. Liquids

It might at first sight seem surprising that nanomaterials could enhance the properties of conventional liquid electrolytes used in rechargeable lithium batteries, yet there is now good evidence for such enhancement. The addition of powders, especially in nanoparticulate form, of compounds such as Al_2O_3, SiO_2, and ZrO_2 to non-aqueous electrolytes can enhance the conductivity by a factor of six (Figure 17).[53]

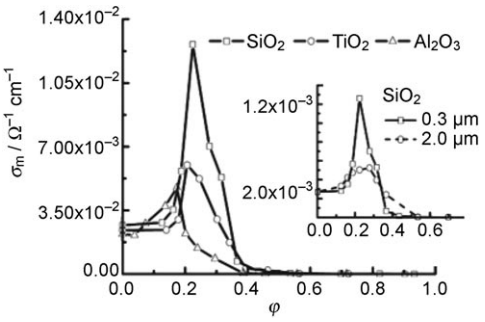

Figure 17. Variation of composite conductivity versus volume fraction (ϕ) of various oxides (particle size, $2r \approx 0.3$ µm) with different surface acid-base character, at room temperature. For all these oxides, conductivity behavior comprises approximately three regimes: a) colloidal regime ($0 < \phi < 0.2$) with low enhancements; b) "soggy sand" ($0.2 < \phi < 0.5$), the regime with the highest conductivities; and c) "dry sand", where the composite exhibits lower conductivities compared to the non-aqueous solution (0.1 M $LiClO_4$ in MeOH). Inset: Influence of SiO_2 particle sizes (size, $2r \approx 0.3$ µm, 2.0 µm) on composite conductivity. Reproduced from reference [53].

The anisotropic forces at the interface between the liquid electrolyte and solid particles are inevitably different from those isotropic forces acting within the bulk of either medium. Space-charge and dipole effects will exist at the interface, leading to changes in the balance between free ions and ion pairs, and hence in the conductivity. Generally, such effects will be enhanced by specific adsorption (chemisorption), for example of the anions on the particle surface, also promoting ion-pair dissociation. Mobility across the surface may also be enhanced. The larger the surface-to-volume ratio (that is, the smaller the particles), the greater the effect per unit mass of powder. Provided there is a sufficient proportion of powder to ensure percolation from one surface to the other, enhanced local conductivity can lead to enhanced long-range conduction through the electrolyte. Because of the quantity of powder required and its resultant mechanical properties, these materials have been termed "soggy sands".

4.2. Amorphous Polymer Electrolytes

Progress in lithium battery technology relies on replacement of the conventional liquid electrolyte by an advanced solid polymer electrolyte.[54,55] To achieve this goal, many lithium-conducting polymers have been prepared and characterized.[56] However, the greatest attention has undoubtedly been focused on poly(ethylene oxide)-based (PEO-based) solid polymer electrolytes.[57] These electrolytes, which are formed by the combination of PEO and a lithium salt, LiX, are often referred as true solid polymer electrolytes (SPEs) as they do not contain plasticizing solvents, and their polymer

chains act at the same time as structural and solvating agents.[58,59]

PEO-based SPEs have a series of specific features, such as low cost, good chemical stability, and safety. However, there are also problems associated with these materials. Their conductivity is high only at temperatures exceeding 70 °C, which narrows the range of practical application for the related polymer battery. In addition, conductivity is due mainly to motion of the anion (the lithium transference number is generally low, of the order of 0.2–0.4) and may result in concentration polarization limiting the rate (power) of the battery.

Accordingly, many attempts have been made to overcome these drawbacks. An interesting approach, which leads to an important enhancement of the transport properties of the PEO-based SPEs, is based on dispersion within the polymer matrix of nanoparticulate ceramic fillers, such as TiO_2, Al_2O_3, and SiO_2.[60] There are obvious analogies with the addition of nanoparticles to liquid electrolytes (amorphous polymers are viscous liquids) although there are also important differences. This new class of SPEs has been referred to as nano composite polymer electrolytes (NCPEs). It has been demonstrated that one of the roles of the filler is that of acting as a solid plasticizer for PEO, by inhibiting chain crystallization upon annealing in the amorphous state at 70 °C.[61,62] This inhibition leads to stabilization of the amorphous phase at lower temperatures and thus to an increase in the useful range of electrolyte conductivity. Furthermore, the ceramic filler promotes enhancement of the lithium-ion transference number, associated with the Lewis acid–base interactions occurring between the surface of the ceramic and both the X^- anion of the salt and the segments of the PEO chain.[4,63]

With a few exceptions, these effects have been confirmed by many laboratories. The degree of enhancement depends on the choice of the ceramic filler and, in particular, of the nature of its surface states. This has been demonstrated by results obtained on a sulfate-promoted superacid zirconia (S-ZrO_2) ceramic filler.[64] The treated zirconia has an acid strength more than twice that of H_2SO_4, associated with the coordinatively unsaturated Zr^{4+} cations, which have a high electron-accepting ability, the latter being enhanced by the nearness of the charge withdrawing sulfate groups.[65,66] Thus, at the surface of the oxide, a high density of acidic sites are present which are of both Lewis and Brønsted type.

Owing to its high acidity, this S-ZrO_2 ceramic material proved an ideal candidate to test the model. Indeed, its dispersion in the classic polymer electrolyte, PEO-$LiBF_4$, has lead to a NCPE having unique transport properties. The transference number, T_{Li^+}, determined using the classical method of Bruce and Vincent, resulted in a T_{Li^+} value of 0.81 ± 0.05; that is, a value almost 100% greater than that of the ceramic-free electrolyte (0.42 ± 0.05).[67,68]

It is important to point out that the development of polymer electrolytes that conduct only cations and are solvent free is considered of prime importance in order to progress lithium batteries. Attempts, mainly directed toward immobilization of the anion in the polymer structure, have been reported in the past, however with modest success, as this approach generally depresses the overall electrolyte conductivity.[69] The nanocomposite approach appears to be more effective, as in this case, the dispersion of an appropriate ceramic filler enhances the lithium transference number without inducing a drastic depression in the electrolyte conductivity. This enhancement is demonstrated in Figure 18 which compares the Arrhenius plots for an electrolyte containing S-ZrO_2 filler and the same electrolyte without filler.[68] Clearly, the conductivity of the electrolyte containing S-ZrO_2 is higher than that without over the entire temperature range.

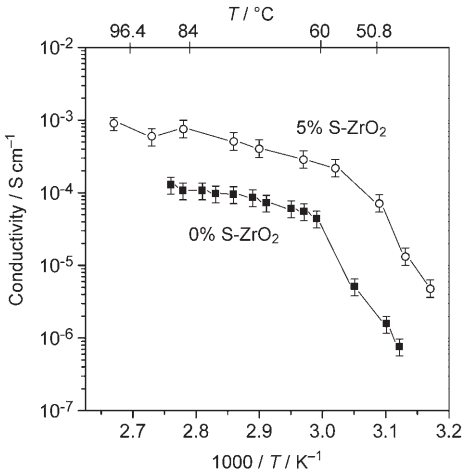

Figure 18. Conductivity Arrhenius plots of composite S-ZrO_2-added electrolyte and of a S-ZrO_2-free electrolyte, both based on the same PEO_8LiBF_4 combination. From reference [62].

The improved performance of a lithium-ion battery composed of a polymer electrolyte containing a nanofiller is shown in Figure 19.[70] Comparison is made between cells containing the $PEO_{20}LiClO_4$ electrolyte with and without S-ZrO_2. Clearly, the battery using the optimized NCPE exhibits a higher cycling capacity, a lower capacity decay upon cycling, and in particular, a more stable charge–discharge efficiency. The last of these points provides clear evidence of another advantage of NCPEs, that is, a less reactive lithium–electrolyte interface.[70]

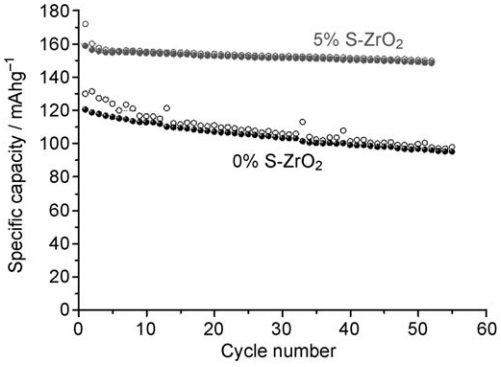

Figure 19. Capacity versus charge-discharge cycles for the Li/$P(EO)_{20}LiClO_4 + 5\%$ S-ZrO_2/$LiFePO_4$ battery (upper curve) and the Li/$P(EO)_{20}LiClO_4$/$LiFePO_4$ battery (lower curve). Temperature: 90 °C. Rate: C/7. The capacity values refer to the cathode. From reference [64].

4.3. Crystalline Polymer Electrolytes

Recent studies have shown that salts, such as $LiXF_6$, where X = P, As, Sb, may be dissolved in solid polymers, such as poly(ethylene oxide) $[(CH_2CH_2O)_n]$, forming crystalline complexes that can support ionic conductivity.[71] In contrast, the established view for 25 years was that crystalline polymer electrolytes were insulators, and conduction occurred only in the amorphous state above the glass transition temperature T_g.[56,72] Such a view was the basis for the results presented in Section 4.2. The crystalline complex composed of six ether oxygen atoms per lithium, poly(ethylene oxide)$_6$:$LiXF_6$, X = P, As, Sb, possesses a crystal structure in which the poly(ethylene oxide) chains form tunnels within which the lithium ions may migrate (Figure 20).[73,74] The use of short poly(ethylene oxide) chains in the nanometer range is essential to avoid the chain entanglement that would occur for longer chains and would inhibit crystallization. Furthermore, for chains in the nanometer range, varying the chain length has an important influence on the conductivity. Reducing the average chain lengths from 44 ethylene oxide units (molar mass approximately 2000, average chain length approximately 90 Å) to 22 ethylene oxide units (molar mass 1000, average chain length of 45 Å) increases the room-temperature conductivity by three orders of magnitude (Figure 21).[73] It is not only important to control the average chain length within the nanometer range but also its dispersity. Polydisperse chain lengths are normally obtained from the chain propagation reactions used to synthesize polymers; these polydisperse chains give rise to higher conductivity than do the equivalent monodisperse materials (Figure 22).[74] The origin of the nanometer effects lies in the fact that the average chain length is much shorter than the crystalline size (2000–2500 Å). As a result, there are many chain ends within each crystallite. They are a natural source of defects, for example, promoting missing lithium ions because of incomplete coordination by the outer oxygen atoms at the chain ends. Shorter chains and polydispersity result in a higher concentration of defects.[74]

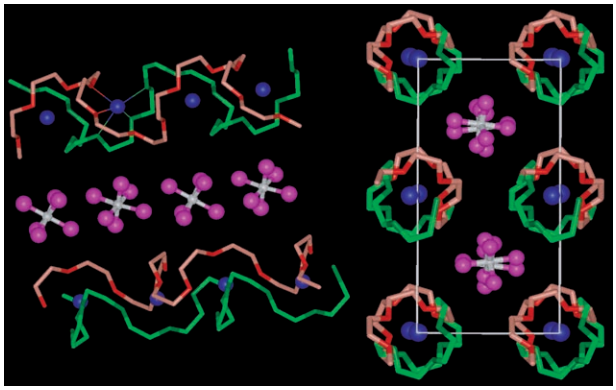

Figure 20. The structure of PEO_6:$LiAsF_6$. Right: view of the structure along the chain axis, showing rows of lithium ions perpendicular to the page. Left: view of the structure showing the relative position of the chains and their conformation (hydrogen atoms not shown). Blue Li, white As, purple F, light green C in chain 1, dark green O in chain 1, pink C in chain 2, red O in chain 2. Thin lines indicate coordination around the lithium ion.

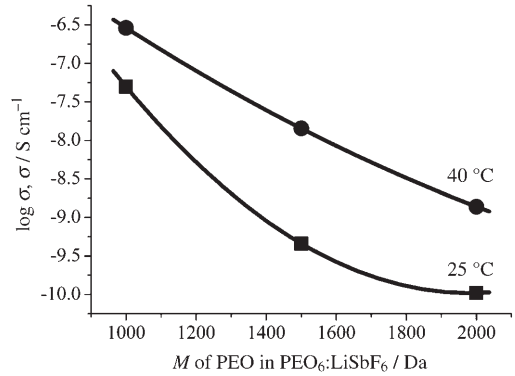

Figure 21. Conductivity isotherms as a function of molecular weight of PEO in PEO_6:$LiSbF_6$.

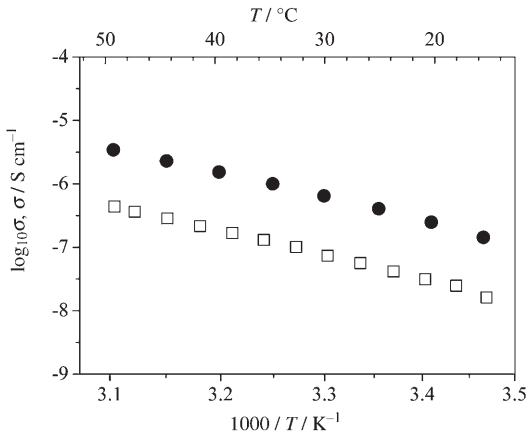

Figure 22. Ionic conductivity of crystalline PEO_6:$LiPF_6$ complexes prepared with mono- (open squares) and polydisperse PEO (solid circles).

5. Positive Electrodes

5.1. Nanoparticles

Most of the lithium intercalation compounds suitable for use as positive electrodes in rechargeable lithium batteries have been prepared in the form of nanoparticles by methods such as grinding, synthesis from solution, or by sol–gel approaches. The rate of lithium intercalation/deintercalation is increased for compounds such as $LiCoO_2$, $LiMn_2O_4$, $Li(Ni_{1/2}Mn_{1/2})O_2$, $Li(Mn_{1/3}Co_{1/3}Ni_{1/3})O_2$, and $Li[Ni_{1/2}Mn_{3/2}]O_4$, because of the shorter diffusion lengths and higher electrolyte/electrode contact area compared with micrometer particles. However, the materials are sufficiently oxidizing to promote decomposition of the electrolyte and formation of a significant solid electrolyte interface layer on the surface of the particles, leading to fade in charge storage.[75,76] Even if such problems of instability could be addressed by more stable electrolytes, there remains the issue, in common with

anode materials, of maintaining good electronic contact between nanoparticles as they expand and contract on intercalation/deintercalation.

Nanoparticulate $LiFePO_4$ deserves special attention.[77] It is an attractive cathode because of its low cost, high thermal and chemical stability, and lower voltage (3.4 V versus Li^+/Li) compared to other positive electrodes, making it less reactive towards electrolytes, resulting in higher electrochemical stability. The intercalation mechanism involves a two-phase reaction between $FePO_4$ and $LiFePO_4$. On extraction of lithium from a particle of $LiFePO_4$, a shell of $FePO_4$ forms just below the surface of the particle, and as lithium continues to be extracted, the phase boundary between this shell and the $LiFePO_4$ core moves through the particle (Figure 23).[78]

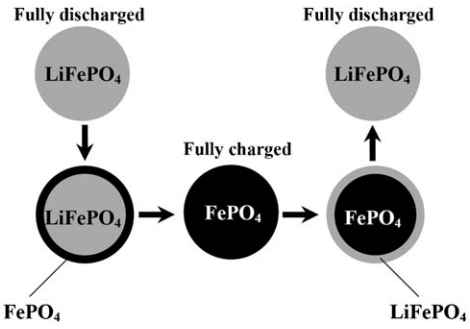

Figure 23. Schematic representation of the processes during charge/discharge of $LiFePO_4$.

Unlike solid-solution electrodes, the potential remains invariant (3.4 V),which is a consequence of the constant chemical potential difference. Each phase is highly stoichiometric with a very low concentration of mixed-valence states and hence poor electronic conductivity. Intercalation/deintercalation from micrometer-sized powders is slow and restricted in extent. However, reducing the particle size to the nanoscale enhances the rate capability to levels of practical utility.[79,80] In some cases, the nanoparticles are painted with a conducting coat; for example, carbon with a high proportion of sp^2 linkages, ensuring good electronic transport between the particles.[81a] Recent studies show that $LiFePO_4$ nanoparticles exhibit a wider range of non-stoichiometry (solid solution) than the micrometer-sized particles, and this non-stoichiometry may in part be responsible for the enhanced rate of lithium intercalation.[81b]

5.2. Nanostructured Positive Electrodes

To avoid the problems encountered with nanoparticulate electrodes, such as poor particle contact or reactive surfaces, but retain the advantages of the nanoscale, attention has turned to nanostructured positive electrodes.

5.2.1. Nanodomain Structures

Starting from the layered intercalation host $LiMnO_2$ (α-$NaFeO_2$ structure), removal of 50% of the lithium induces a conversion to the spinel structure, involving displacement of 25% of the manganese ions from the transition-metal layers into octahedral sites in the neighboring alkali metal layers, whereas lithium is displaced into tetrahedral sites in the alkali metal layers.[82] It is possible for the manganese and lithium ions to occupy the cubic close-packed oxide subarray in two ways (lithium in 8a and manganese in 16d, or lithium in 8b and manganese in 16c; space group $Fd\bar{3}m$), both corresponding to a spinel structure, leading to the nucleation and growth of spinel nanodomains within the micrometer-sized particles (Figure 24).[82–84]

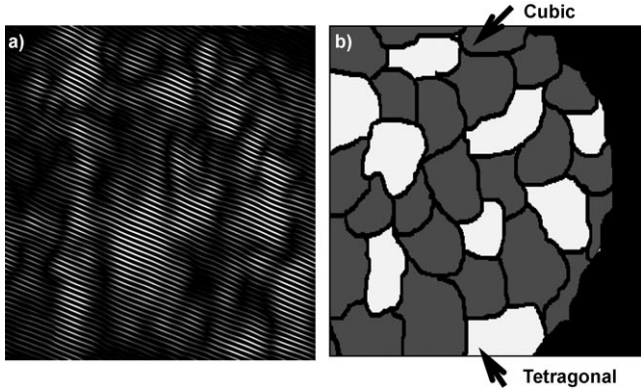

Figure 24. a) TEM image of nanostructured $LiMn_2O_4$ spinel obtained on cycling layered $LiMnO_2$. Fourier-filtered image highlights the nanodomain structure of average dimensions 50–70 Å. b) A schematic representation of the nanodomain structure of $LiMn_2O_4$ spinel derived from layered $LiMnO_2$, showing cubic and tetragonal nanodomains.

$LiMn_2O_4$ spinel is a lithium intercalation host with the ability to vary its composition over the range $Li_xMn_2O_4$, $0 < x < 2$. For the composition range $0 < x < 1$, the structure is cubic. For $1 < x < 2$, the Mn^{3+} (high spin $3d^4$) occupancy exceeds the critical 50% required to induce a cooperative Jahn–Teller distortion and a lowering of the overall symmetry from cubic to tetragonal.[85] As a result, on cycling lithium over the composition range $0 < x < 2$, the system passes between cubic and tetragonal structures. In the case of $LiMn_2O_4$ without a nanodomain structure, the nucleation and growth of the Jahn–Teller distorted phase on cycling lithium results in poor reversibility (Figure 25a).[86] However, in the case of the nanodomain structure, entire domains can spontaneously switch between cubic and tetragonal structures on lithium insertion/removal, with the associated 13% anisotropic change of lattice parameters being accommodated by slippage at the domain wall boundaries (Figure 24).[82,87,88] This mechanism leads to a dramatic improvement in the retention of capacity on cycling compared with the normal spinel material (Figure 25b). Subsequently, it was shown that by grinding normal $LiMn_2O_4$, a similar nanodomain structure could be induced within the particles, leading to a comparable improvement in the ability to cycle lithium.[89]

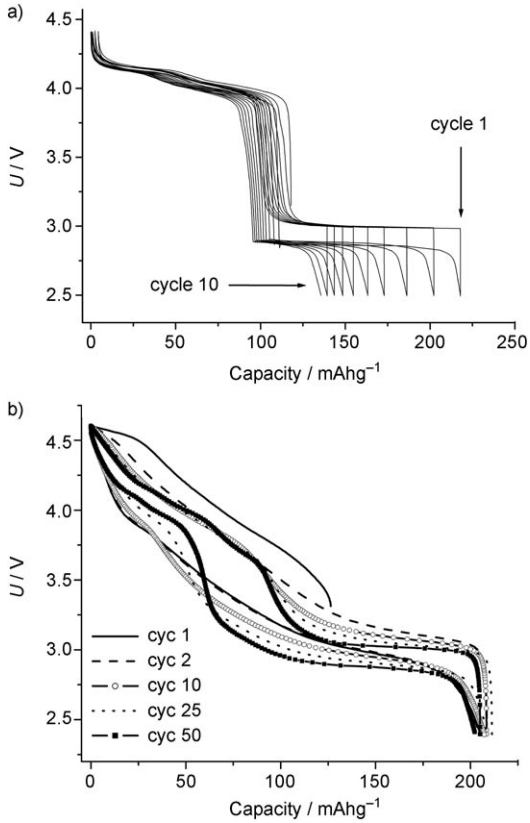

Figure 25. Variation of potential with state of charge (lithium content) on cycling (a) $Li_{1.07}Mn_{1.93}O_4$ spinel prepared by high-temperature solid-state reaction and (b) nanostructured $Li_xMn_2O_4$ spinel formed in situ from layered $LiMnO_2$, rate = 25 mAg^{-1} (ca. *C*/8, that is, discharge in 8 h).

5.2.2. *Nanotubes/wires*

As described for anodes, it is possible to fabricate nanostructured positive electrodes of various dimensions, most notably nanowires or nanotubes. For example, nanotubes of V_2O_5 and nanowires of other lithium intercalation hosts, including $LiCoO_2$ and $Li(Ni_{1/2}Mn_{1/2})O_2$, have been prepared, and shown to act as intercalation hosts for lithium.[90–92] In many cases, the performance, especially in terms of rate capability, is enhanced compared with bulk materials.

5.2.3. *Ordered Mesoporous Materials*

One approach to new positive electrode materials capable of more rapid intercalation/deintercalation, and hence higher power, than the materials used presently, is to synthesize ordered mesoporous solids. Such materials are composed of micrometer-sized particles within which pores of diameter 2–50 nm exist.[93] The pores are of identical size, and are ordered such that the thickness of the walls between the pores are the same throughout the particles (typically 2–8 nm). Because the particles are of micrometer dimensions, the materials may be fabricated into cathodes using the same screen-printing techniques used currently for $LiCoO_2$ rechargeable lithium batteries. Furthermore, the micrometer-sized particles will exhibit similar packing to that of conventional powders, and hence the electrical contact between particles will be similar. However, the internal pores can be flooded with electrolyte, ensuring a high surface area in contact with the electrode and hence a high flux of lithium across the interface. Also, unlike the porosity that exists between particles in an electrode, the size of which is random and highly distributed, the uniformity of pore size and regularity in the arrangement of the pores (ordered porosity) ensures an even distribution of electrolyte in contact with the electrode surface. The thin walls, of equal dimensions throughout, ensure short diffusion paths for lithium ions on intercalation/deintercalation, and hence equal, high, rates of transport throughout the material.

Ordered mesoporous solids based on silicas, and other main-group solids, are well known. Studies of mesoporous transition-metal oxides are less well developed, in part because of the greater difficulty in synthesizing such materials. As all the lithium in a lithium-ion cell originates from the cathode, ordered mesoporous cathodes must be based on lithium transition-metal compounds, presenting an even greater challenge to synthesis. Recently, the first example of an ordered mesoporous lithium transition-metal oxide, the low temperature (LT) polymorph of $LiCoO_2$, has been synthesized and shown to exhibit superior properties as a cathode compared with the same compound in nanoparticulate form. Transmission electron micrographs of the resulting mesoporous LT-$LiCoO_2$ are shown in Figure 26.[91] The pores are ordered in three dimensions, with a pore size of 40 Å and wall thickness of 70 Å. Synthesis involves using a mesoporous silica with a 3D pore structure, such as KIT-6, as a template. A soluble cobalt source is dissolved in water and impregnated into the pores of the mesoporous silica. Heating results in formation of Co_3O_4 inside the pores. By dissolving the silica template, a replica structure of mesoporous Co_3O_4 remains,

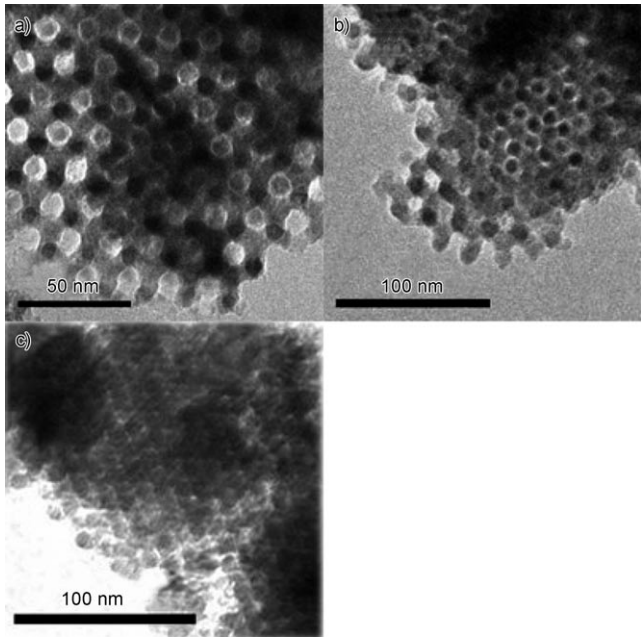

Figure 26. TEM images of (a) as-prepared mesoporous Co_3O_4, (b) mesoporous LT- $LiCoO_2$, and (c) mesoporous LT-$LiCoO_2$ after 200 cycles.

which is then reacted in the solid state with LiOH to form LT-$LiCoO_2$ (Figure 26).[91a] Crucially, the ordered mesoporous structure is retained during conversion of Co_3O_4 to LT-$LiCoO_2$ (Figure 26). A comparison of the cycling performance of an electrode formed from mesoporous LT-$LiCoO_2$ and nanoparticulate powder of the same material with a similar surface area (70 $m^2 g^{-1}$ and 40 $m^{-2} g^{-1}$ respectively) is shown in Figure 27. These results indicate that the ordered

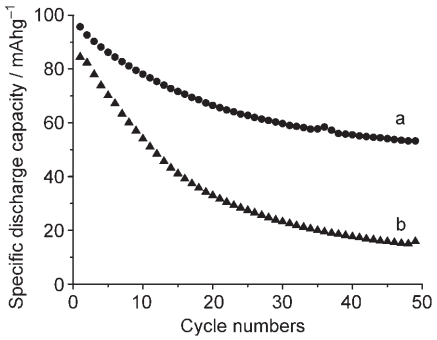

Figure 27. Charge storage (lithium) as a function of cycle number for (a) mesoporous LT-$LiCoO_2$ and (b) nanoparticle LT-$LiCoO_2$.

mesoporous material demonstrates superior lithium cycling during continuous intercalation/removal. The origin of this effect lies in the better particle contact of the micrometer-sized particles, better electrolyte access via the ordered pore structure, and the short diffusion distances for lithium ions and electrons within the walls. It may also be the case that the surface of the pores has a lower reactivity compared with the external surface of the LT-$LiCoO_2$ nanoparticles in contact with the same electrolyte. LT-$LiCoO_2$ is not in itself an exceptional positive electrode, but it does serve to demonstrate the potential advantages gained by synthesizing positive electrodes in the form of ordered mesoporous materials. Very recently, Bruce et al. demonstrated the synthesis of mesoporous $LiMn_2O_4$.[91b] As a bulk phase, $LiMn_2O_4$ possesses the best rate performance of any positive electrode. The mesoporous form exhibits even better rate capability, with a higher capacity to store charge at high rate than the bulk phase, whether cycled over 4 V or both 3 and 4 V plateaus (Figure 28). Ordered mesoporous forms of more significant intercalation electrodes will be seen in the future.

Although the main focus of this Review concerns the formation of nanostructured powders, important work has also been carried out on the growth of nanostructured materials directly on electrode substrates. For example, compounds such as NiOOH have been grown using liquid crystalline electrolytes as a structure-directing medium for the electrochemical growth of this material on an electrode substrate.[94,95] Clearly similar approaches can and have been taken to the growth of other materials.

5.2.4. *Disordered Porous Positive Electrodes*

A number of materials have been prepared with high internal surface areas, for which the porosity is distributed in

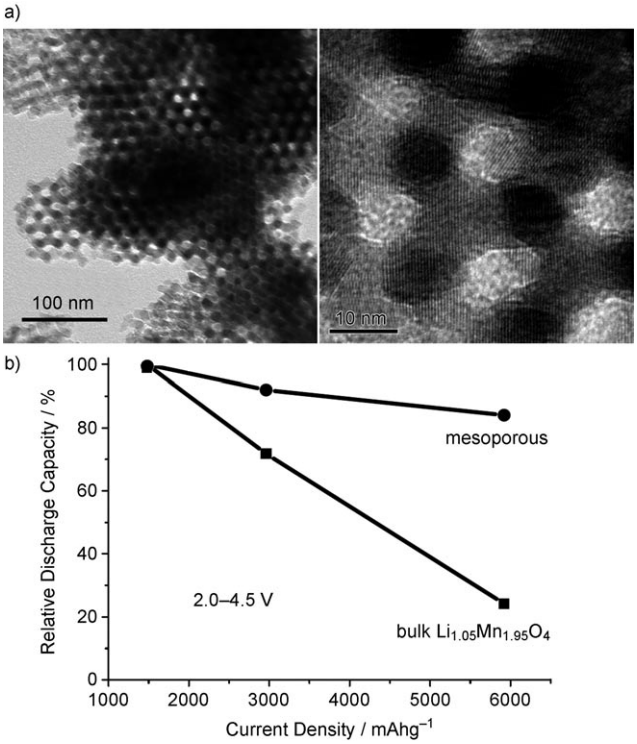

Figure 28. a) TEM images of mesoporous $LiMn_2O_4$, b) comparison of capacity retention as a function of rate between the best bulk and mesoporous lithium manganese oxide spinels cycled over 3 and 4 V plateaus.

shape and size. Synthesis usually involves starting with a solution phase, followed by condensing, oxidizing, or reducing the transition-metal centers to form extended networks, from which water may be removed to form aero- or xerogels. Aerogels are of primary interest in this area because of their high surface area. Such materials have an enhanced rate capability compared with dense micrometer-scale powders, and the reactivity of their internal surfaces may differ from the same compounds prepared as nanoparticles. Aerogels often retain some water, which is considered by some authors to represent a disadvantage for their use in non-aqueous lithium-ion batteries. Amongst the materials that have been investigated are V_2O_5, MnO_2, and Li_xMnO_2.[96–98] An advantage of these materials is that their preparation can, in some instances, be straightforward compared with the formation of the more ordered mesoporous materials.

Although not a nanomaterial, it is appropriate to mention briefly macroporous solids to place the other materials in context. Starting with latex beads of monodisperse dimensions around 400–500 nm, it is possible to arrange such beads in an ordered array, and impregnate the space between the beads with a solution precursor, which can then be converted to form a lithium transition-metal oxide. This procedure has been carried out for $LiCoO_2$ and $LiNiO_2$.[99,100] Following heating to remove the latex beads, pores of circa 500 nm remain. These materials provide ready access for electrolyte, but of course also compromise the amount of active material per unit volume, and hence the volumetric energy density, to an even greater degree than mesoporous materials.

6. Three-Dimensional Batteries with Nanostructured Electrodes

Conventional rechargeable lithium batteries consist of electrodes that provide sufficient porosity between the particles to allow electrolyte to penetrate between them, thus forming a three-dimensional interface. The 3D concept can be extended to the whole cell. Just as in large cities, where architects extend buildings in the 3rd dimension to increase density, so too can materials electrochemists to increase volumetric energy density.[101]

Another example of where 3D configurations can be beneficial is the field of microbatteries, especially as microelectronics is constantly demanding more power from less space on the chip. Today's solid state lithium or lithium-ion thin-film batteries with their flat, 2D configuration falls short of meeting the needs of emerging MEMS devices. The microelectronics industry has outpaced advances in small-scale power supplies. The present state of the art 2D-microbatteries can deliver maximum capacity, energy, and power of 10 μA h, 3.6 μW h, and 180 μW mm^{-2}, respectively.[102] The need for greater performance within less space is encouraging investigation of the 3D microbattery concept. Calculations indicate an increase in performance by at least a factor of four over the 2D counterparts.[103,104]

Numerous 3D-architectures are under consideration.[105] Some are based on the deposition of electrodes/electrolytes around two interpenetrating arrays of carbon rods.[103] Others rely on the simple use of vertical "posts" connected to a substrate, wherein the layered battery structure is formed around the posts.[106] Making such 3D structures relies presently on the use of either costly micro- and photolithography techniques, or electrodeposition techniques combined with spin coating/infiltration; making three consecutive layers by electrodeposition is not feasible because the electrolyte component is electronically insulating. To overcome some of these technical barriers, Peled's group recently developed a new assembly concept based on the use of a porous silicon substrate, and reported the first working 3D thin-film microbattery.[107,108] The battery is formed within the micropores of the substrate using several steps:

1) Electroless deposition of a nickel current collector
2) the electrochemical deposition of the cathode
3) the addition of the polymer electrolyte by sequential spin-coating and vacuum pulling
4) the filling, with an infiltration process, of the remaining holes by graphite.

This structure delivers a large capacity increase compared with state-of-the-art thin-film microbatteries with the same footprint (5 mA h cm^{-2} vs. 0.25 mA h cm^{-2}) while offering excellent lifetime and power (rate) capability. An innovative alternative fabrication method for 3D batteries, based on the use of a heterogeneous colloid to define the 3D architecture, has also been reported.[109] Such positive attributes for 3D nanostructured electrodes compared with planar structures in terms of capacity and power was described above in Section 3.5 for the conversion reaction with Fe_3O_4 electroplated on a copper–nanorod alloy (Figure 29).[49,110]

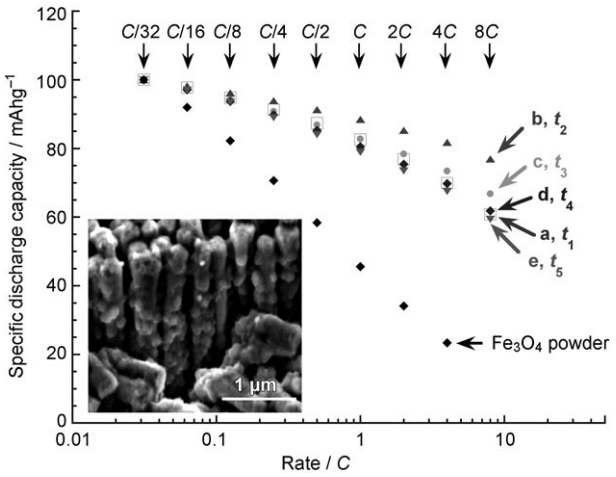

Figure 29. Specific discharge capacity vs. rate plot comparing the rate of 3D-nanoarchitectured Fe_3O_4 electrode with 2D-Fe_3O_4 planar electrodes having the same footprint. Electrodes lettered a)–e) were obtained by progressively increasing the deposition time from 120 s (a) to 300 s (e). The inset shows an SEM micrograph of the electrode with the copper nanorods supporting crystals of the electrodeposited Fe_3O_4 phase.

Although the benefits of 3D batteries have been clearly demonstrated, the main difficulties lie in finding simple, low cost assembly processes. One promising approach is to form the battery on a single foam sponge electrode; such an approach is being pursued by several research groups.

7. Supercapacitors and Fuel Cells

The advantages of using nanomaterials are not limited to lithium batteries, but also apply to other electrochemical devices, such as supercapacitors and fuel cells. Supercapacitors and batteries have a similar configuration, that is, two electrodes separated by an electrolyte, but the former are designed for high power and long life service. Recent trends involve the development of high-surface-area nanostructured carbon electrodes to enhance capacitance and power delivery. These materials include aerogels, nanotemplated carbon, and carbon nanotubes. Significant improvements in performance have been obtained, although the optimum compromise between surface area (to ensure high capacitance) and pore-size distribution (to allow easy access to the electrolyte) has yet to be achieved.

The practical development of fuel cells relies to a great extent on nanotechnology. The use of high-surface-area carbon supports helps to achieve a fine dispersion of the precious metal catalyst, which itself is of nanoparticle size. Examples of carbon supports are carbon nanofibers, carbon aerogels, or mesoporous carbons. By following this approach, reduction in the platinum content to significantly less than 0.5 mg cm^{-2} without degrading the cell performance and lifetime has been demonstrated for polymer-electrolyte membrane fuel cells (PEMFCs); that is, the fuel cell which is presently considered the most promising for application in hydrogen-fuelled, low-emission vehicles. A more detailed

discussion of supercapacitors and fuel cells, including the use of nanomaterials, is beyond the scope of this Review, but may be found in the cited papers.[4,111]

8. Summary and Outlook

This Review demonstrates that the chemistry of nanomaterials is important for future research into rechargeable lithium batteries. The significance of nanomaterials is demonstrated by their incorporation, in the form of nanoparticles, into the latest commercial rechargeable lithium batteries; for example, nano-$LiFePO_4$ cathodes and tin–carbon alloy anodes. To store more energy in the anode, new nanoalloys (Section 3.3) or displacement reactions (Section 3.4), or conversion reactions (Section 3.5) will be required. The Review also highlights the important advantages of nanostructured materials, as opposed to simple nanoparticulate materials. For example, the superior properties of TiO_2 nanowires and mesoporous $LiCoO_2$ are discussed in Sections 3.2 and 5.2.3, respectively. Future generations of rechargeable lithium batteries that can exhibit higher energy and higher power will depend crucially on the use of nanostructured materials as electrodes and electrolytes (for example, heterogeneous doping of amorphous polymers, see Section 4.2). The ultimate expression of the nanoscale in rechargeable lithium batteries is the formation of 3D nanoarchitectured cells, in which pillared anodes and cathodes are interdigitated. Such novel architectures, which can lead to higher energy densities, will be an important feature of research in future years.

The authors would like to thank Dr. Allan Paterson for his assistance with the preparation of some of the figures.

Received: June 8, 2007
Published online: March 12, 2008

[1] *Advances in Lithium-ion Batteries* (Eds.: W. van Schalkwijk, B. Scrosati), Kluwer Academic/Plenum, New York, **2002**.
[2] *Lithium Batteries Science and Technology* (Eds.: G.-A. Nazri, G. Pistoia), Kluwer Academic/Plenum, Boston, **2004**.
[3] M. S. Whittingham, *Chem. Rev.* **2004**, *104*, 4271.
[4] A. S. Aricò, P. Bruce, B. Scrosati, J.-M. Tarascon, W. Van Schalkwijc, *Nat. Mater.* **2005**, *4*, 366.
[5] F. Jiao, P. G. Bruce, *Adv. Mater.* **2007**, *19*, 657.
[6] P. Balaya, A. J. Bhattacharyya, J. Jamnik, Y. F. Zhukovskii, E. A. Kotomin, J. Maier, *J. Power Sources* **2006**, *159*, 171.
[7] N. Meethong, H.-Y. S. Huang, W. C. Carter, Y.-M. Chiang, *Electrochem. Solid-State Lett.* **2007**, *10*, A134.
[8] E. Peled, *J. Electrochem. Soc.* **1979**, *126*, 40.
[9] R. Fong, V. von Schen, J. R. Aohn, *J. Electrochem. Soc.* **1990**, *137*, 2009.
[10] R. Hanno, Y. Kawamdo, *J. Electrochem. Soc.* **1992**, *139*, 3397.
[11] R. S. Morris, B. G. Dixon, T. Gennett, R. Raffaelle, M. J. Heben, *J. Power Sources* **2004**, *138*, 277.
[12] Z. Zhou, J. J. Zhao, X. P. Gao, Z. F. Chen, J. Yan, P. V. Schiever, M. Morinaga, *Chem. Mater.* **2005**, *17*, 992.
[13] E. Ferg, R. J. Gummow, A. Dekock, M. M. Thackeray, *J. Electrochem. Soc.* **1994**, *141*, L147.
[14] A. N. Jansen, A. J. Kahalan, K. D. Kepler, P. A. Nelson, K. Amine, D. W. Dees, D. R. Vissers, M. M. Thackeray, *J. Power Sources* **1999**, *81*, 902.
[15] P. Reale, S. Panero, B. Scrosati, J. Garche, M. Wohlfahrt-Mehrens, M. Wachtler, *J. Electrochem. Soc.* **2004**, *151*, A2138.
[16] A. R. Armstrong, G. Armstrong, J. Canales, P. G. Bruce, *Angew. Chem.* **2004**, *116*, 2336; *Angew. Chem. Int. Ed.* **2004**, *43*, 2286.
[17] A. R. Armstrong, G. Armstrong, J. Canales, R. Garcia, P. G. Bruce, *Adv. Mater.* **2005**, *17*, 862.
[18] A. R. Armstrong, G. Armstrong, J. Canales, P. G. Bruce, *Chem. Commun.* **2005**, 2454.
[19] G. Armstrong, A. R. Armstrong, P. G. Bruce, P. Reale, B. Scrosati, *Adv. Mater.*, **2006**, *18*, 2597.
[20] M.-S. Park, G.-X. Wang, Y.-M. Kang, D. Wexler, S.-X. Dou, H.-K. Liu, *Angew. Chem.* **2007**, *119*, 764; *Angew. Chem. Int. Ed.* **2007**, *46*, 750.
[21] C. K. Chan, H. L. Peng, R. D. Twesten, K. Jarausch, X. F. Zhang, Y. Cui, *Nano Lett.* **2007**, *7*, 490.
[22] K. T. Nam, D.-W. Kim, P. J. Yoo, C.-Y. Chiang, N. Meethong, P. T. Hammond, Y.-M. Chiang, A. M. Belcher, *Science* **2006**, *312*, 885.
[23] M. Winter, J. O. Besenhard, *Electrochim. Acta* **1999**, *45*, 31.
[24] R. A. Huggins in *Lithium Batteries* (Eds.: G.-A. Nazri, G. Pistoia), Kuwer Academic, Boston, **2004**, p. 270.
[25] H. Mukaibo, T. Osaka, P. Reale, S. Panero, B. Scrosati, M. Wacthler, *J. Power Sources* **2004**, *132*, 225.
[26] I. Amadei, S. Panero, B. Scrosati, G. Cocco, L. Schiffini, *J. Power Sources* **2005**, *143*, 227.
[27] H. Mukaibo, T. Sumi, T. Yokoshima, T. Momma, T. Osaka, *Electrochem. Solid-State Lett.* **2003**, *6*, A218.
[28] J. Hassoun, S. Panero, B. Scrosati, *J. Power Sources* **2006**, *160*, 1336.
[29] M. Green, E. Fielder, B. Scrosati, M. Wachtler, J. Serra Moreno, *Electrochem. Solid-State Lett.* **2003**, *6*, A75.
[30] A. Timons, J. Li, J. Dahn, IMLB 2006, Biarritz, France, June 18–23, **2006**, Abstract 229.
[31] P. L. Taberna, S. Mitra, P. Piozot, P. Simon, J. M. Tarascon, *Nat. Mater.* **2006**, *5*, 567.
[32] a) J. Hassoun, S. Panero, P. Simon , P. L. Taberna, B. Scrosati, *Adv. Mater.* **2007**, *19*, 1632; b) A. Timmons, J. R. Dahn, *J. Electrochem. Soc.* **2007**, *154*, A444.
[33] K. Nakajima, Batteries 2006, 6–8th June, Paris, France.
[34] H. Inoue, IMLB 2006, Biarritz, France, June 18–23, 2006, Abstract 228.
[35] K. D. Kepler, J. T. Vaughey, M. M. Thackeray, *Electrochem. Solid-State Lett.* **1999**, *2*, 307.
[36] a) M. M. Thackeray, *Nat. Mater.* **2002**, *1*, 81; b) L. M. L. Fransson, J. T. Vaughey, R. Benedek, K. Edstrom, J. O. Thomas, M. M. Thackeray, *Electrochem. Commun.* **2001**, *3*, 317.
[37] J. Thomas, *Nat. Mater.* **2003**, *2*, 201.
[38] N. Ravet, J. B. Goodenough, S. Besner, M. Simoneau, P. Hovington, M. Armand, *Improved iron-based cathode material*, ECS Fall meeting, Hawai Abstract N°127, **1999**.
[39] M. Morcrette, P. Rozier, L. Dupont, E. Mugnier, L. Sannier, J. Galy, J. M. Tarascon, *Nat. Mater.* **2003**, *2*, 755.
[40] P. Poizot, S. Laruelle, S. Grugeon, L. Dupont, J.-M. Tarascon, *Nature* **2000**, *407*, 496.
[41] P. Poizot, S. Laruelle, S. Grugeon, L. Dupont, B. Beaudoin, J.-M. Tarascon, *C. R. Acad. Sci. Ser. IIc* **2000**, *3*, 681.
[42] N. Pereira, L. Dupont, J. M. Tarascon, L. C. Klein, G. G. Amatucci, *J. Electrochem. Soc.* **2003**, *150*, A1273.
[43] H. Li, G. Richter, J. Maier, *Adv. Mater.* **2003**, *15*, 736.
[44] F. Badway, N. Pereira, F. Cosandey, G. G. Amatucci, *J. Electrochem. Soc.* **2003**, *150*, A1209.
[45] B. Bervas, F. Badway, L. C. Klein, G. G. Amatucci, *Electrochem. Solid-State Lett.* **2005**, *8*, A179.

[46] D. C. C. Silva, O. Crosnier, G. Ouvrard, J. Greedan, A. Safa-Sefat, L. Nazar, *Electrochem. Solid-State Lett.* **2003**, *6*, A162.
[47] V. Pralong, D. C. S. Souza, K. T. Leung, L. Nazar, *Electrochem. Commun.* **2002**, *4*, 516.
[48] P. Poizot, S. Laruelle, S. Grugeon, L. Dupont, J. M. Tarascon, *Ionics* **2000**, *6*, 321.
[49] P. L. Taberna, S. Mitra, P. Poizot, P. Simon, J. M. Tarascon, *Nat. Mater.* **2006**, *7*, 567.
[50] J.-M. Tarascon, S. Grugeon, S. Laruelle, D. Larcher, P. Poizot in *Lithium Batteries—Science and Technology* (Eds.: G. A. Nazri, G.Pistoia), Kluwer Academic Publishers, Boston, **2003**, chap. 7.
[51] S. Grugeon, S. Laruelle, L. Dupont, F. Chevallier, L. Gireaud, P. L. Taberna, P. Simon, B. Yrieix, E. Vidal, S. Lascaud, J. M. Tarascon, *Chem. Mater.* **2005**, *17*, 5041.
[52] F. Gillot, S. Boyanov, L. Dupont, M. L. Doublet, M. Morcrette, L. Monconduit, J. M. Tarascon, *Chem. Mater.* **2005**, *17*, 6327.
[53] J. Bhattacharyya, J. Maier, *Adv. Mater.* **2004**, *16*, 811.
[54] F. Grey, *Solid Polymer Electrolytes*, VCH, Weinheim, **1991**.
[55] See ref. [1].
[56] B. Scrosati, *Chem. Rec.* **2005**, *5*(5), 286.
[57] C. A. Vincent, B. Scrosati, *Bull. Mater. Res. Soc.* **2000**, *25*, 28.
[58] F. Grey, M. Armand in *Handbook of Battery Materials* (Ed.: J. O. Besenhard), Wiley-VCH, Weinheim, **1999**, p. 499.
[59] *Handbook of Battery Materials* (Ed.: J. O. Besenhard), Wiley-VCH, Weinheim, **1999**.
[60] F. Croce, G. B. Appetecchi, L. Persi, B. Scrosati, *Nature* **1998**, *394*, 456.
[61] F. Croce, R. Curini, A. Martinelli, L. Persi, F. Ronci, B. Scrosati, *J. Phys. Chem. B* **1999**, *103*, 10632.
[62] F. Croce, B. Scrosati, *Ann. N. Y. Acad. Sci.* **2003**, *984*, 194.
[63] G. B. Appetecchi, F. Croce, L. Persi, L. Ronci, B. Scrosati, *Electrochim. Acta* **2000**, *45*, 1481.
[64] F. Croce, L. Settimi, B. Scrosati, *Electrochem. Commun.* **2006**, *8*, 364.
[65] R. J. Gillespie, *Acc. Chim. Res.* **1968**, *1*, 202.
[66] V. Bolis, G. Magnaccia, G. Cerrato, C. Morterra, *Langmuir* **1997**, *13*, 888.
[67] P. G. Bruce, J. Evans, C. A. Vincent, *Solid State Ionics* **1988**, *28*, 918.
[68] F. Croce, L. Settimi, B. Scrosati, *Electrochem. Commun.* **2006**, *8*, 364.
[69] J. B. Kerr in *Lithium Batteries, Science and Technology* (Eds.: G. A. Nazri, G. Pistoia), Kluwer Academic, Dordrecht, **2003**, p. 602.
[70] F. Croce, S. Sacchetti, B. Scrosati, *J. Power Sources* **2006**, *162*, 685.
[71] Z. Gadjourova, Y. Andreev, D. P. Tunstall, P. G. Bruce, *Nature* **2001**, *412*, 148.
[72] A. M. Christie, S. J. Lilley, E. Staunton, Y. G. Andreev, P. G. Bruce, *Nature* **2005**, *433*, 50.
[73] Z. Stoeva, I. Martin-Litas, E. Staunton, Y. G. Andreev, P. G. Bruce, *J. Am. Chem. Soc.* **2003**, *125*, 4619.
[74] E. Stanton, Y. G. Andreev, P. G. Bruce, *Faraday Discuss.* **2007**, *134*, 143.
[75] H. K. Liu, G. X. Wang, Z. P. Guo, J. Z. Wang, K. Konstantinov, *J. Nanosci. Nanotechnol.* **2006**, *6*, 1.
[76] S. H. Ye, J. Y. Lv, W. P. Gao, F. Wu, D. Y. Song, *Electrochim. Acta* **2004**, *49*, 162.
[77] A. K. Padhi, K. S. Nanjundaswamy, C. Masquelier, S. Okada, J. B. Goodenough, *J. Electrochem. Soc.* **1997**, *144*, 1609.
[78] V. Srinivasan, J. Newman, *Electrochem. Solid-State Lett.* **2006**, *9*, A110.
[79] H. Huang, S-C. Yin, L. F. Nazar, *Electrochem. Solid-State Lett.* **2001**, *4*, A170.
[80] C. Delacort, P. Poizot, S. Levasseur, C. Masquelier, *Electrochem. Solid-State Lett.* **2006**, *9*, A352.
[81] a) A. Ravet, Y. Chouinard, J. F. Magnan, S. Besner, M. Gauthiér, M. Armand, *J. Power Sources* **2001**, *97*, 503; b) N. Meethong, H. Y. S. Huang, W. C. Carter, Y. M. Chiang, *Electrochem. Solid-State Lett.* **2007**, *10*, A134.
[82] P. G. Bruce, A. R. Armstrong, R. Gitzendanner, *J. Mater. Chem.* **1999**, *9*, 193.
[83] A. D. Robertson, A. R. Armstrong, A. J. Fowkes, P. G. Bruce, *J. Mater. Chem.* **2001**, *11*, 113.
[84] A. R. Armstrong, A. J. Paterson, A. D. Robertson, P. G. Bruce, *Chem. Mater.* **2002**, *14*, 710.
[85] M. M. Thackeray, W. I. F. David, P. G. Bruce, J. B. Goodenough, *Mater. Res. Bull.* **1983**, *18*, 461.
[86] A. D. Robertson, A. R. Armstrong, P. G. Bruce, *Chem. Mater.* **2001**, *13*, 2380.
[87] Y. Shao-Horn, S. A. Hackney, A. R. Armstrong, P. G. Bruce, R. Gitzendanner, C. S. Johnson, M. M. Thackeray, *J. Electrochem. Soc.* **1999**, *146*, 2404.
[88] H. F. Wang, Y. I. Jang, Y.-M. Chiang, *Electrochem. Solid-State Lett.* **1999**, *2*, 490.
[89] S. H. Kang, J. B. Goodenough, L. K. Rabenberg, *Chem. Mater.* **2001**, *13*, 1758.
[90] S. Nordlinder, L. Nyholm, T. Gustafsson, K. Edstrom, *Chem. Mater.* **2006**, *18*, 495.
[91] a) F. Jiao, K. M. Shaju, P. G. Bruce, *Angew. Chem.* **2005**, *117*, 6708; *Angew. Chem. Int. Ed.* **2005**, *44*, 6550; b) F. Jiao, P. G. Bruce, submitted.
[92] Y. K. Zhou, H. L. Li, *J. Mater. Chem.* **2002**, *12*, 681.
[93] J. D. Epping, B. F. Chonelka, *Curr. Opin. Colloid Interface Sci.* **2006**, *11*, 81.
[94] K. H. Reiman, K. M. Brace, T. J. Gordon-Smith, I. Nandhakumar, G. S. Attard, J. R. Owen, *Electrochem. Commun.* **2006**, *8*, 517.
[95] P. A. Nelson, J. R. Owen, *J. Electrochem. Soc.* **2003**, *150*, A1313.
[96] B. B. Owens, S. Passerini, W. H. Smyrl, *Electrochim. Acta* **1999**, *45*, 215.
[97] J. Kim, A. Manthiram, *Electrochem. Solid-State Lett.* **1998**, *5*, 207.
[98] P. E. Tang, J. S. Sakamoto, E. Baudrin, B. Dunn, *J. Non-Cryst. Solids* **2004**, *350*, 67.
[99] H. W. Yan, S. Sokolov, J. C. Lytle, A. Stein, F. Zhang, W. H. Smyrl, *J. Electrochem. Soc.* **2003**, *150*, A1102.
[100] G. A. Armstrong, P. G. Bruce, personal communication **2006**.
[101] J. Lee, J. Kim, *J. Microelectromech. Syst.* **2000**, *9*, 71.
[102] G. Nagasubramanian, D. H. Doughty, *J. Power Sources* **2004**, *136*, 395.
[103] R. W. Hart, H. S. White, B. Dunn, D. R. Rolison, *Electrochem. Commun.* **2003**, *5*, 120.
[104] C. L. Wang, L. Taherabadi, G. Y. Jia, M. Madou, Y. T. Yeh, B. Dunn, *Electrochem. Solid-State Lett.* **2004**, *7*, A435 – A438.
[105] B. Dunn, *Chem. Rev.* **2003**, *104*, 4463.
[106] A. Singh, J. Jarayan, M. Madou, S. Akhbar, *J. Electrochem. Soc.* **2002**, *149*, E78.
[107] M. Nathan, D. Haronian, E. Peled, US Patent No. 6,197,450, **2004**.
[108] M. Nathan, D. Golodnisky, V. Yufit, E. Strauss, T. Ripenbein, I. Shechtman, S. Menkin, E. Peled, *J. MELS* **2005**, *14*, 879.
[109] Y. K. Cho, R. Wartena, S. M. Tobias, Y.-M. Chiang, *Adv. Funct. Mater.* **2007**, *17*, 379.
[110] P. L. Taberna, P. Simon, J. M. Tarascon, French Patent No. 0,504,960, **2006**.
[111] Y. Shao, G. Yin, Z. Wang, Y. Gao, *J. Power Sources* **2007**, *167*, 235.

